

## Augmented-plane-wave calculation of indirect-exchange matrix elements for gadolinium\*

B. N. Harmon

Ames Laboratory-U.S.AEC and Department of Physics, Iowa State University, Ames, Iowa 50010

A. J. Freeman

Physics Department, Northwestern University, Evanston, Illinois 60201  
and Argonne National Laboratory, Argonne, Illinois 60439

(Received 22 May 1974; revised manuscript received 14 August 1974)

The exchange matrix elements between a local  $4f$  moment and the conduction electrons (Ruderman-Kittel-Kasuya-Yosida exchange) have been calculated for paramagnetic gadolinium metal using nonrelativistic augmented-plane-wave wave functions. The magnitude of the matrix elements is found to be largest for  $d$ -like conduction electrons and is quite sensitive to their angular distribution. Because of band crossings, which cause rapid changes in wave-function character, the matrix elements cannot be well described as slowly varying functions of  $\vec{q} = \vec{k}' - \vec{k}$ .

### I. INTRODUCTION

The exchange interaction between the localized  $4f$  electrons and the conduction electrons is basic for understanding the electric, magnetic, and optical properties of the rare-earth metals<sup>1</sup> (and for a variety of physical problems such as local moments in dilute alloys, Kondo effect,<sup>2</sup> etc.<sup>3</sup>). The net spin from the open  $4f$ -shell electrons plays an essential role in promoting magnetic ordering through the mechanism of indirect exchange between the localized and the conduction-band electrons. This indirect-exchange mechanism produces an effective  $4f$ - $4f$  coupling which is responsible for the various observed magnetic properties. (The direct-exchange interaction between  $4f$  electrons on different sites is too small to play a significant role in accounting for the strong magnetic ordering observed because the  $4f$  wave functions on different atomic sites have negligible overlap.) First proposed by Ruderman and Kittel<sup>4</sup> to explain the effective long-range coupling between nuclear spins interacting via the Fermi hyperfine interaction, this mechanism was later extended by Kasuya<sup>5</sup> and Yosida<sup>6</sup> to treat local-moment-conduction-electron interactions in magnetic materials and is now referred to as the Ruderman-Kittel-Kasuya-Yosida (RKKY) interaction.

In the rare earths,<sup>1</sup> the  $4f$  electrons overlap the conduction electrons and their net spin polarizes the conduction electrons via the exchange interaction. Unlike the Coulomb interaction which is periodic and does not scatter the conduction electrons, the nonlocal exchange interactions are not periodic and do scatter the conduction electrons when the spin directions of the open-shell electrons are disturbed. This spin-disorder scattering gives rise to the resistivity in first order. It is the second-

order process which is responsible for the effective spin-spin interaction between the open-shell electrons and gives rise to the magnetic ordering (i. e., the resultant conduction-electron polarization from a single ion is carried over to the vicinity of other ions and will interact via the same exchange interaction with their  $4f$  shells and produce an alignment of the moments). In Gd the  $4f$  electrons have zero orbital angular momentum, and the basic spin-dependent Hamiltonian between the local moments and conduction electrons is well known,<sup>5</sup>

$$\mathcal{H}_{c..-f}(\vec{R}_i) = -\frac{1}{N} \sum_{\vec{k}, \vec{k}'} I_{nn'}(\vec{k}, \vec{k}') \times e^{i(\vec{k}-\vec{k}') \cdot \vec{R}_i} [(a_{\vec{k}n}^* + a_{\vec{k}',n'} + a_{\vec{k}n}^* - a_{\vec{k}',n'}) S_i^z + a_{\vec{k}n}^* + a_{\vec{k}',n'} - S_i^- + a_{\vec{k}n}^* - a_{\vec{k}',n'} + S_i^+], \quad (1)$$

where  $\vec{S}_i$  is the spin on the localized ion located at  $\vec{R}_i$ , and  $N$  is the number of unit cells in the crystal. The  $a_{hno}^*$  and  $a_{hno}$  are the creation and annihilation operators for an electron in the Bloch state with wavevector  $\vec{k}$ , band index  $n$ , and spin  $\sigma$ .  $I_{n,n'}(\vec{k}, \vec{k}')$  is the matrix element for the exchange coupling of local states with the conduction electrons. This Hamiltonian is also approximately applicable to the other rare-earth metals if  $\vec{S}_i$  is replaced by the de Gennes factor  $(g-1)\vec{J}$  (Ref. 7); however, the presence of the orbital contribution to the localized moment can lead to anisotropic interactions as shown by Kaplan and Lyons.<sup>8</sup> Estimates of these anisotropic corrections for free electrons indicate that they may be quite important.<sup>8,9</sup> In this paper we will be concerned with only the isotropic Hamiltonian which is valid for Gd and will express our results for the matrix elements in

terms of

$$j_{n,n'}(\vec{k}, \vec{k}') = 7I_{n,n'}(\vec{k}, \vec{k}') \quad (2)$$

where

$$j_{n,n'}(\vec{k}, \vec{k}') = N \sum_{m=-3}^{+3} \int \int \psi_{\vec{k},n}^*(\vec{r}_1) \Phi_{4f,m}^*(\vec{r}_2) \times (2/r_{12}) \Phi_{4f,m}(\vec{r}_1) \psi_{\vec{k}',n'}(\vec{r}_2) d\vec{r}_1 d\vec{r}_2. \quad (3)$$

Since the seven unpaired 4*f* electrons of gadolinium constitute a half-closed shell, the sum of their distributions is spherically symmetric and only the

$$J(\vec{R}_{ij}) = \frac{4}{N^2} \sum_{\vec{k}, \vec{k}', n, n'} |I_{n,n'}(\vec{k}, \vec{k}')|^2 \frac{e^{i(\vec{k}-\vec{k}') \cdot \vec{R}_{ij}} f_{n,\vec{k}} (1-f_{n',\vec{k}'})}{E_{n'}(\vec{k}') - E_n(\vec{k})}, \quad (4)$$

where  $\vec{R}_{ij} = \vec{R}_i - \vec{R}_j$  and  $f_{n,\vec{k}}$  and  $f_{n',\vec{k}'}$  are the Fermi distribution functions.<sup>1</sup>

The evaluation of the RKKY interaction has only been possible by making some extreme approximations. The conduction-electron states have commonly been taken as plane waves and the free-electron Fermi surface used; however, augmented-plane-wave (APW) energy-band calculations<sup>1,10</sup> have shown that these metals have transition-metal band structures with strongly hybridized *s-p* and *d* bands. More recent investigations have taken the band structures into account, but they have not included the actual matrix elements.<sup>1,11</sup> These later calculations have been primarily concerned with relating the magnetic ordering to the "nesting features" found on the complicated Fermi surfaces. These calculations ignore the matrix elements in Eq. (4) and rely on the assumption that the dominant structure in the 4*f*-4*f* interaction is caused by the complicated energy dependence of the denominator. While these calculations have been successful in explaining the relationship of the Fermi-surface geometry to the magnetic ordering, they cannot supply the details of the interaction; thus, experimental quantities like the magnon spectrum [the Fourier transform of Eq. (4) if the band splitting is ignored] have not been obtained from first-principles calculations. Basic to these calculations are the exchange-matrix elements, Eq. (3), which contain the details of the 4*f*-conduction-electron interaction.

Many approximations for the matrix elements have been made in order to facilitate calculations. The assumption that  $j_{n,n'}(\vec{k}, \vec{k}') = j = \text{const}$  seemed reasonable for the nuclear coupling problem originally considered by Ruderman and Kittel<sup>4</sup> because a  $\delta$ -function interaction between a nucleus and plane waves yields  $j = \text{const}$ . As a better approximation, since the matrix elements depend sensitively on  $|\vec{k} - \vec{k}'|$ , it has been assumed that  $j(\vec{k}, \vec{k}')$

same angular components of  $\psi_{\vec{k}}$  and  $\psi_{\vec{k}'}$  will be coupled.

To describe the coupling of the 4*f* electrons located at different sites the  $\mathcal{J}_{c.o.-f}$  interaction must be taken to second order. The coupling may be considered as the interaction of a local moment on one site giving rise to the virtual excitation of an electron  $\vec{k}$  into an empty state  $\vec{k}'$  which then interacts with a local moment on another site. The exchange interaction between two spins located at lattice sites *i* and *j* is given by

depends only on  $\vec{k}' - \vec{k} = \vec{q}$ . Overhauser assumed that the Coulomb interaction in Eq. (3) was so strongly shielded that it could be replaced by a  $\delta$  function.<sup>12</sup> With plane waves this results in a  $j(\vec{q})$  which is simply the form factor (i.e., the Fourier transform) of the local-moment density.

Kaplan and Lyons pointed out that for the rare earths  $j(\vec{q})$  would not be well approximated by a constant, even for plane waves,<sup>8</sup> while Kaplan suggested that the  $(\vec{k}, \vec{k}')$  dependence may be important.<sup>13</sup> In several investigations, Watson and Freeman calculated first<sup>14,15</sup> the behavior of  $j(\vec{k}, \vec{k}')$  when assumed to be of the approximate form  $j(\vec{q})$  and then the  $(\vec{k}, \vec{k}')$  dependence of  $j(\vec{k}, \vec{k}')$  for an in-structure model. They found some important differences between the two sets of results for  $j(\vec{k}, \vec{k}')$  and for the induced conduction-electron spin polarization. For their calculations, they used the illustrative case of a spherical local moment which consisted of the half-filled shell of  $\text{Gd}^{3+}(4f^7)$  and conduction electrons which were represented by a single plane wave orthogonalized to both the closed shell and 4*f* electrons. Analytic atomic Hartree-Fock wave functions were used for the  $\text{Gd}^{3+}$  ion. Their results showed that there was a strong  $(\vec{k}, \vec{k}')$  dependence, that the even simpler RKKY and Overhauser approximations were too crude, and that accurate calculations using energy-band wave functions for the metals were required to determine the true nature of  $j(\vec{k}, \vec{k}')$ . The importance of the  $(\vec{k}, \vec{k}')$  dependence was also noted by Mahanti and Das,<sup>16</sup> who used a single orthogonalized-plane-wave (OPW) approach based on real band structures and found the  $(\vec{k}, \vec{k}')$  dependence of the hyperfine matrix elements important for understanding experimental results for Rb and Cs.

This paper reports on a study of the exchange interactions between the localized 4*f* electrons and the conduction-band electrons in Gd metal. Both diagonal and off-diagonal matrix elements  $j_{n,n'}(\vec{k}, \vec{k}')$

have been determined using energy-band wave functions determined from an augmented-plane-wave calculation for the paramagnetic state of the metal. Gadolinium was chosen for several reasons. It is the simplest rare-earth metal to consider since the ground-state  $4f$  moment is spherically symmetric ( $^8S$  state) and is uncomplicated by orbital-moment contributions. Since the net spin of the gadolinium  $4f$  electrons is the largest of the rare earths, the exchange interaction with the conduction electrons should yield the largest experimental consequences (e. g. band splitting). In addition, the magnon dispersion curves of gadolinium have been measured<sup>17</sup> [which gives essentially the Fourier transform of  $J(\vec{R}_{ij})$ ], an accurate neutron magnetic form factor has been obtained<sup>18</sup> [which has given direct information about both the local moment<sup>19</sup> and itinerant (conduction) electron-spin distributions<sup>20</sup>], and optical-absorption measurements<sup>21</sup> may be used to compare with a special case of our calculated results.

## II. METHOD OF CALCULATION

All electronic energy-band structures which have been reported for the rare-earth metals have been obtained by the APW method; gadolinium in particular has been studied in detail in both the nonrelativistic<sup>1,12,22</sup> and relativistic<sup>23</sup> approximations. Recently we have reported<sup>20</sup> on a detailed study of the spin-polarized energy-band structure, conduction-electron polarization and neutron magnetic form factor of ferromagnetic Gd metal. We found that the conduction-electron spin density determined from the APW wave functions is mostly of  $d$  character and emphasized the possible role of these electrons in the interactions responsible for ferromagnetism in the metal.

In the present work we have used the APW method to determine the energy-band structure and wave functions for the paramagnetic state. We are concerned with obtaining normalized wave functions, and have therefore employed the linearized form of the APW method.<sup>24</sup> Since the APW method is well known, we give only those basic details necessary for understanding the calculation of  $j_{n,\nu}(\vec{k}, \vec{k}')$ . The crystal potential  $V(r)$  was obtained by using the usual<sup>25</sup> prescription of superposing atomic charge densities from neighboring sites and using the full Slater  $\rho^{1/3}$  exchange. The atomic densities were determined from a self-consistent Hartree-Fock-Slater calculation with the assumed atomic configuration  $4f^7 5d^1 6s^2$ . Eigenvalues and eigenfunctions for paramagnetic Gd metal were determined at 125 points in the irreducible  $\frac{1}{24}$  of the Brillouin zone. The points were located in five horizontal planes at the positions shown in Fig. 1. The planes were located in  $\pi/5c$  increments from  $\pi/10c$  to  $9\pi/10c$ . The basis set used for a particular  $\vec{k}$

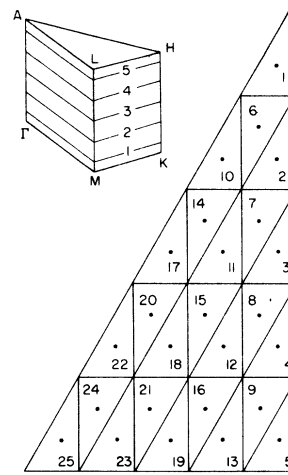


FIG. 1. Irreducible  $\frac{1}{24}$  of the Brillouin zone for the Hexagonal lattice, and a horizontal plane showing the points at which wave functions and matrix elements were evaluated. For matrix elements with  $\vec{q} = q_{\pi} + 0$  there is no reflection symmetry in the  $z=0$  plane so that wave functions were actually evaluated on ten such planes and at 250 total points.

point in the Brillouin zone was determined by including all those reciprocal lattice vectors  $\vec{k}_i$  that satisfied the relation  $|\vec{k} + \vec{k}_i| r_{MT} \leq 7.0$ , where  $r_{MT}$  is the muffin-tin radius (3.2080 a. u.). This procedure results, typically, in 70 to 80 basis functions and a convergence of better than 2 mRy on the eigenvalue. The APW wave-function convergence has been discussed previously<sup>26</sup> and will not be repeated here.

In calculating the matrix elements we obtained the  $4f$  orbitals for the crystal potential and found it convenient to expand the APW Bloch states inside the muffin-tin spheres as

$$\psi_{n,\vec{k}}(\vec{r}) = \sum_{l,m} A_{lm}(\vec{k}, n) u_{l,E\vec{k}}(r) Y_{lm}(\hat{r}), \quad (5)$$

where

$$u_{l,E\vec{k}}(r) = R_{l,E\vec{k}}(r) / R_{l,E\vec{k}}(r_{MT}), \quad (6)$$

and the  $R_{l,E\vec{k}}(r)$  are obtained by numerically integrating the Schrödinger equation. When it is noted that the  $4f$  orbitals are essentially zero outside the APW sphere, the exchange integral of Eq. (3) is easily evaluated inside the sphere by using the same procedures as are used in atomic Hartree-Fock calculations.<sup>27</sup> We have found that only terms up to  $l=3$  need be included in the wave-function expansion of Eq. (5) for the precise (better than 1%) calculation of the matrix elements.

## III. RESULTS

To obtain an idea of the magnitude of the contribution from each  $l$  component of the wave function,

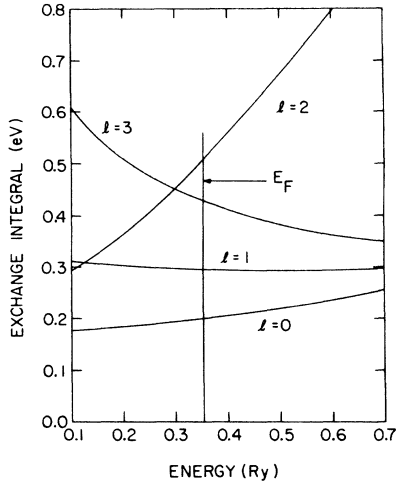


FIG. 2. Diagonal radial exchange integral  $I_l(E, E)$  of Eq. (7). The integral reflects the overlap of the different  $l$  radial functions with the  $4f$  orbitals.

we can take the Bloch functions as having pure- $l$  character about each atomic site and ignore the  $k$  dependence; thus

$$\Psi_{l,E}(\vec{r}) = u_{l,E}(r)Y_{l,m}(\hat{r})$$

The  $u_{l,E}(r)$  functions are obtained by integrating the radial Schrödinger equation and are normalized such that

$$\int_0^{R_{ws}} u_{l,E}^2(r) r^2 dr = \frac{1}{2}$$

Here  $R_{ws}$  is the Wigner-Seitz sphere radius, and the  $\frac{1}{2}$  comes from there being two atoms per unit cell in the hcp structure. Equation (3) is then evaluated using these "wave functions" to obtain

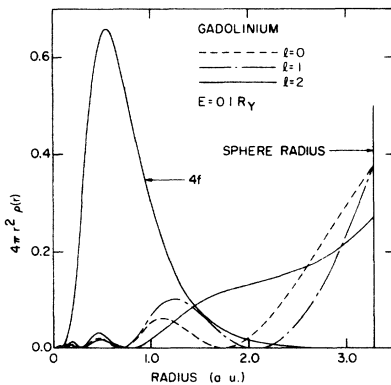


FIG. 3. Radial density of the different  $l$  components of the wave functions at  $E=0.1$  Ry. The radial functions have been normalized to  $\frac{1}{2}$  inside the Wigner-Seitz sphere. The  $4f$  eigenvalue is  $-0.55$  Ry. The  $4f$  function has also been normalized to  $\frac{1}{2}$  instead of 7 for convenience in plotting the figure.

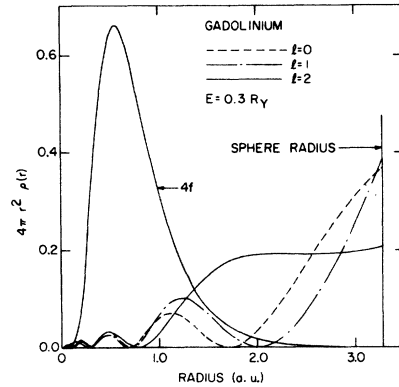


FIG. 4. Radial densities for  $E=0.3$  Ry.

$$I_l(E, E') = \sum_{\mu} \iint \Psi_{l,E}^*(\vec{r}_1) \Phi_{4f,\mu}^*(\vec{r}_2) (2/r_{12}) \times \Phi_{4f,\mu}(\vec{r}_1) \Psi_{l,E'}(\vec{r}_2) d\vec{r}_1 d\vec{r}_2. \quad (7)$$

The integral for  $E=E'$ , i. e., the diagonal part of the matrix element of Eq. (7), is shown in Fig. 2. The  $4f$  exchange with the conduction-band  $l=3$  radial function is seen to be quite large; however, there is less than 3%  $l=3$  character to any of the wave functions we obtained so that the total  $l=3$  contributions to the exchange integrals were usually less than 8%.

In Eq. (4), those states near the Fermi surface with  $(\vec{k} - \vec{k}') \cdot \vec{R}_{ij}$  nearly stationary are most heavily weighted.<sup>28</sup> We have found all states on or very near the Fermi surface to have 80 to 95%  $l=2$  character, with  $l=1$  character making up most of the remainder. This combination of  $l=1$  and  $l=2$  character in the wave functions near the Fermi energy produces a large  $l=3$  nonspherical contribution to the spin density,<sup>20</sup> which has relevance for the observed neutron magnetic form factor.<sup>18</sup> (The  $l=4$  radial integral, not shown in Fig. 2, is on the order of  $10^{-3}$  eV throughout the entire energy range and is therefore negligible.)

Figures 3–5 show how the different  $l$  radial functions change as the energy increases. The bottom of the  $s$ -like conduction band (at  $\Gamma$ , in the Brillouin zone) occurs near  $E=0.1$  Ry. At  $E=0.3$  Ry the  $d$  bands are beginning to be occupied and have a very diffuse density. Above the Fermi energy ( $E_F = 0.353$  Ry), the bands are unoccupied, and the  $l=2$  function becomes more contracted—finally resembling an atomic  $5d$  orbital near  $E=0.7$  Ry. These figures give a good intuitive feel as to how the radial-exchange integrals depend on energy. The overlap of the  $l=2$  radial function with the  $4f$  orbital is seen to increase much more rapidly from Fig. 3 to Fig. 5 than the overlap of the  $l=0$  or the  $l=1$  functions. This is the same behavior displayed by the exchange integrals of Fig. 2.

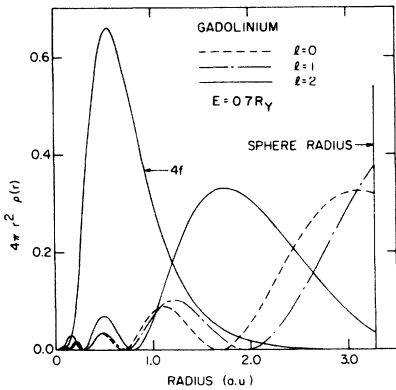


FIG. 5. Radial densities for  $E = 0.7 \text{ Ry}$ .

The  $E'$  dependence of the exchange integral, Eq. (7), for  $E = E_F$  is shown in Fig. 6. From this plot we see that the radial part of the matrix elements does not fall off very rapidly for large energy differences. This means that the sum over bands in Eq. (4) will probably have to be taken over all ten  $d$  bands in order to obtain complete convergence, although contributions from those bands at the Fermi energy (bands 3 and 4) will be the most significant. (This question of the number of bands needed for convergence will be discussed with the calculation of the magnon-dispersion curves.<sup>29</sup>)

Since the magnetic-ordering structures observed in the heavy rare-earth metals can be described by a wave vector along the  $\Gamma$  to  $A$  direction in the Brillouin zone, we have calculated the matrix elements for  $(\vec{k}' - \vec{k}) = \vec{q} = q_z$  along each of the 25 vertical lines which pass through the points in Fig. 1. As a typical example which demonstrates the general character observed, we have plotted, in Fig. 7, bands 3 and 4 and the corresponding  $q$

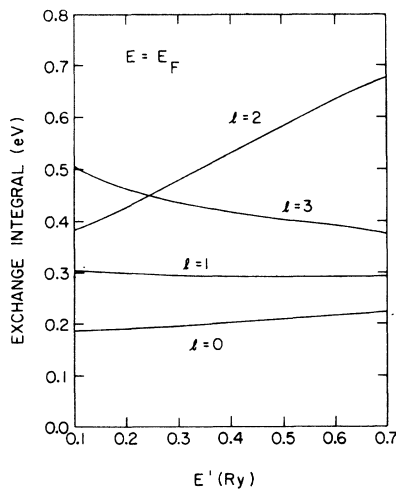


FIG. 6. Radial exchange integral  $I_l(E_f, E')$  of Eq. (7), showing the  $E'$  dependence.

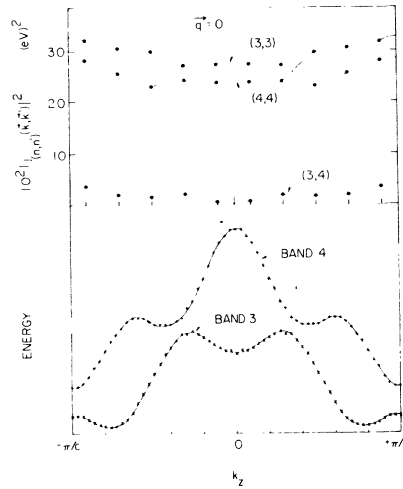


FIG. 7. Third and Fourth bands along the vertical line which passes through point 2 in Fig. 1. The corresponding  $q=0$  matrix elements are shown vertically above these bands, for both intraband and interband "transitions."

$= 0$  intraband and interband matrix elements for the vertical line passing through the point labeled 2 in Fig. 1. To easily obtain a global representation of the bands, the eigenvalues were least-squares fitted using symmetrized plane waves (rms error = 2 mRy). The errors in the fitting at the AHL plane are the reason for the approximately 5-mRy gap between the third and fourth band at  $k_z = \pm \pi/c$ . The wave functions of both bands are  $d$ -like and thus have about the same magnitude for the intraband matrix elements. The interband matrix elements are very small because the angular distribution of the wave functions is nearly orthogonal [i. e., the  $A_{2m}$ 's of Eq. (5) cause the matrix element to be small]. For  $q \neq 0$  the wave function's coupling bands 3 and 4 need no longer be of different angular distribution; therefore large interband matrix elements may occur, as shown in Fig. 8 for  $q = \pi/5c$ . The oscillations are caused by the band crossing which, for  $q \neq 0$ , allows wave functions with similar angular distributions to couple. For the 25 vertical lines and the different  $q$  values we have studied, these oscillations are the rule rather than the exception, so that any analytical arguments based on simplified band structures and wave functions would be doubtful.

If there are no band crossing as one moves horizontally in the Brillouin zone (i. e., keeping  $k_z$  fixed), the variation of the matrix elements is not large, as is shown in Fig. 9. Here we have plotted the matrix elements for  $q = 3\pi/5c$  between bands 3 and 4 along the vertical lines through the neighboring points 9, 13, and 16 of Fig. 1. We should remark here that the curves passing

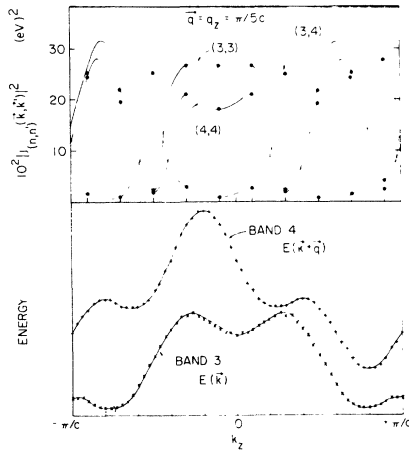


FIG. 8. Matrix elements with  $(\vec{k}' - \vec{k}) = \vec{q} = \pi/5c$  for the same bands as shown in Fig. 7. Band 4 has been plotted so that the corresponding matrix elements are vertically above the bands. There is no reflection symmetry in the  $k_z = 0$  plane.

through these points have been drawn by "eyeball", and the few inbetween points we have checked suggest that the peaks or oscillations may be sharper than we have drawn them but that the lines give a good overall description of the matrix-element variations.

In ferromagnetic gadolinium the spin splitting of the  $n$ th band at  $\vec{k}$  is proportional to the size of the  $4f$ -conduction-electron interaction. The magnitude of the average splitting at the Fermi surface has been determined by two different experiments. In one experiment, optical measurements reveal an apparent absorption between the spin split bands (allowed in the presence of spin-orbit coupling) at the Fermi level and suggest a splitting in the neighborhood of 0.7 eV.<sup>21</sup> This result may not be an accurate average over the Fermi surface, however, since some regions near the surface may contribute more than others due to differences in the magnitude of the optical matrix elements.

The other experiment which gives information about the average splitting is a measurement of the total saturated magnetic moment at low temperature and in a high magnetic field. The measured moment is  $7.55 \mu_B/\text{atom}$ , which is  $0.55 \mu_B/\text{atom}$  above that expected from the seven unpaired  $4f$  electrons.<sup>30</sup> The extra  $0.55 \mu_B/\text{atom}$  comes from the unpaired spin-up electrons near the Fermi level. Assuming a rigid-band model, the amount of splitting needed to produce this moment is easily calculated from the paramagnetic density of the states:

$$\delta n = n_+ - n_-$$

$$= \int_0^{E_F} N(E) dE - \int_0^{E_F} N(E) dE \quad (8)$$

with  $\delta n = 0.55/\text{atom}$  and our calculated density of states (using a histogram increment of 0.002 Ry) we obtained the splitting  $E_{F+} - E_{F-} = 0.56$  eV. The assumption of rigid-band splitting is reasonable since the dominant character of all the eigenstates near the Fermi energy is  $d$ -like, and the splitting in the bands has been found to be proportional to the amount of  $d$  character.<sup>20</sup>

The theoretical magnitude of the band splitting is easily obtained from our matrix-element calculations. In the magnetically ordered state the energy of a spin-up conduction electron of wave vector  $\vec{k}$  and band index  $n$  will differ from the energy of the corresponding spin-down electron by  $2j_{n,n}(\vec{k}, \vec{k})$ ; where  $j_{n,n}(\vec{k}, \vec{k})$  is given in Eq. (3) and the factor of 2 is because there are two  $4f$  moments in each unit cell of the hcp crystal. As a very good approximation we may take the wave-function character for all the states at the Fermi level to be pure  $d$ -like, and obtain from Fig. 2 a value for  $j_{n,n}(\vec{k}, \vec{k})$  of 0.51 eV at  $E = E_F$ . Thus we would predict the band splitting at the Fermi level to be about 1 eV, which is considerably larger than the two values quoted above.

An obvious reason which can be given for the larger theoretical value of the band splitting is the neglect of screening in Eq. (3) for the  $4f$ -conduction-electron exchange. Screening or correlation effects are known to reduce the calculated atomic Hartree-Fock exchange integrals between  $4f$  electrons by about 25% as determined from atomic spectroscopy measurements.<sup>31</sup> In the solid one would expect increased screening from the  $5d$  conduction electrons near the Fermi level. The amount of reduction of the calculated Hartree-Fock conduction-electron- $4f$  interaction caused by

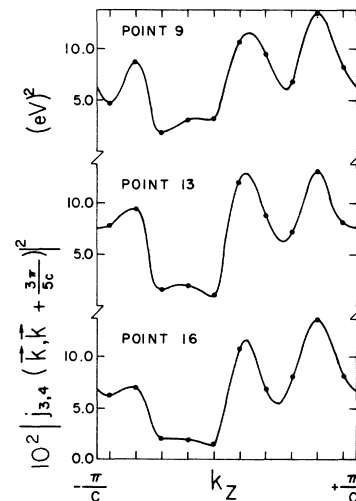


FIG. 9. Interband matrix elements for the three vertical lines passing through the neighboring points 9, 13, and 16 of Fig. 1.

screening is, however, difficult to estimate, but the difference between our calculated value and the experimental values seems reasonable. In the future we hope to study these screening effects in more detail. We do not expect them to change the  $k$  dependence of the matrix elements we have calculated, but rather we expect their main effect will be to scale the magnitude of the matrix elements.

#### IV. CONCLUSIONS

The large  $4f$  exchange interaction with the  $d$ -like electrons and the predominant  $d$  character of the wave functions (80 to 95%) near the Fermi energy indicate that the  $d$ -like electrons play the dominant role in coupling the local  $4f$  moments. Since  $d$  electrons have considerably more angular variations than do  $s$  or  $p$  electrons, the matrix elements are much more complicated than might

be expected if a  $4f$ - $s$  interaction were dominant.

We chose gadolinium because of its spherical distribution of  $4f$  electrons; however, nonspherical  $4f$  distributions are not that much more difficult to handle<sup>8,9</sup> and should provide insight into some of the large anisotropies observed in the other rare-earth metals. These and many other interesting questions can be studied once the matrix elements have been calculated. We hope to report in the near future on some calculations which utilize these matrix elements.<sup>29</sup>

#### ACKNOWLEDGMENT

The authors are indebted to Dale Koelling for many helpful discussions concerning the computational aspects of the problem, and one of us (B. N. H.) would like to thank him for his hospitality at Argonne National Laboratory during his stay there.

- 
- <sup>1</sup>A. J. Freeman, in *Magnetic Properties of Rare Earth Metals*, edited by R. J. Elliott (Plenum, New York, 1972) Chap. 6, and references therein.
- <sup>2</sup>J. Kondo, *Prog. Theor. Phys.* **32**, 37 (1964).
- <sup>3</sup>A. J. Heeger, *Solid State Phys.* **23**, 283 (1969).
- <sup>4</sup>M. A. Ruderman and C. Kittel, *Phys. Rev.* **96**, 99 (1954).
- <sup>5</sup>T. Kasuya, *Prog. Theor. Phys.* **16**, 45 (1956); see also A. H. Mitchell, *Phys. Rev.* **105**, 1439 (1957).
- <sup>6</sup>K. Yosida, *Phys. Rev.* **106**, 893 (1957).
- <sup>7</sup>S. H. Liu, *Phys. Rev.* **121**, 451 (1961).
- <sup>8</sup>T. A. Kaplan and D. H. Lyons, *Phys. Rev.* **129**, 2072 (1963).
- <sup>9</sup>F. Specht, *Phys. Rev.* **162**, 389 (1967).
- <sup>10</sup>J. O. Dimmock and A. J. Freeman, *Phys. Rev. Lett.* **13**, 750 (1964).
- <sup>11</sup>W. E. Evenson and S. H. Liu, *Phys. Rev. Lett.* **21**, 432 (1968); and S. H. Liu, R. P. Gupta, and S. K. Sinha, *Phys. Rev. B* **4**, 1101 (1971).
- <sup>12</sup>A. W. Overhauser, *J. Appl. Phys.* **34**, 1019 (1963), and references therein.
- <sup>13</sup>T. A. Kaplan, *Phys. Rev. Lett.* **14**, 499 (1965).
- <sup>14</sup>R. E. Watson and A. J. Freeman, *Phys. Rev.* **152**, 566 (1966).
- <sup>15</sup>R. E. Watson and A. J. Freeman, *Phys. Rev.* **178**, 725 (1969).
- <sup>16</sup>S. D. Mahanti and T. P. Das, *Phys. Rev.* **170**, 426 (1968).
- <sup>17</sup>W. C. Koehler, H. R. Child, R. M. Nicklow, H. G. Smith, R. M. Moon, and J. W. Cable, *Phys. Rev. Lett.* **24**, 16 (1970).
- <sup>18</sup>R. M. Moon, W. C. Koehler, J. W. Cable and H. R. Child, *Phys. Rev. B* **5**, 997 (1972).
- <sup>19</sup>A. J. Freeman and J. P. Desclaux, *Int. J. Magn.* **3**, 311 (1972).
- <sup>20</sup>B. N. Harmon, Ph.D. thesis (Northwestern University, 1973) (unpublished); B. N. Harmon and A. J. Freeman, *Phys. Rev. B* **10**, 1979 (1974).
- <sup>21</sup>J. N. Hodgson and B. J. Cleyet, *J. Phys. C* **2**, 97 (1969).
- <sup>22</sup>J. O. Dimmock, A. J. Freeman, and R. E. Watson, *J. Appl. Phys.* **36**, 1142 (1965).
- <sup>23</sup>S. C. Keeton and T. L. Loucks, *Phys. Rev.* **146**, 429 (1966); **168**, 672 (1968).
- <sup>24</sup>D. D. Koelling, *J. Phys. Chem. Solids* **33**, 1335 (1972); B. N. Harmon and D. D. Koelling, *J. Phys. C* **7**, L210 (1974).
- <sup>25</sup>L. F. Matthiess, *Phys. Rev.* **133**, 184 (1963).
- <sup>26</sup>B. N. Harmon, D. D. Koelling, and A. J. Freeman, *J. Phys. C* **6**, 2294 (1973).
- <sup>27</sup>D. R. Hartree, *The Calculations of Atomic Structures* (Wiley, New York, 1957).
- <sup>28</sup>L. M. Roth, H. J. Zeiger, and T. A. Kaplan, *Phys. Rev.* **149**, 519 (1966).
- <sup>29</sup>B. N. Harmon, P. Lindgård, A. J. Freeman (unpublished).
- <sup>30</sup>H. E. Nigh, S. Legvold, and F. H. Spedding, *Phys. Rev.* **132**, 1092 (1963).
- <sup>31</sup>A. J. Freeman and R. E. Watson, *Phys. Rev.* **127**, 2058 (1962).